Electronic Supplementary Material (ESI) for Chemical Communications

Supporting Information to Accompany "**A Highly Sensitive Two-Photon Fluorescent Probe for Mitochondrial Zinc Ions in Living Tissue**"

Na Young Baek,[1] Cheol Ho Heo,[1] Chang Su Lim,[2] Goutam Masanta,[3] Bong Rae Cho,*[2] and Hwan Myung Kim*[1,3]

[1]*Molecular Science & Technology Research Center,* [3]*Division of Energy Systems Research, Ajou University, Suwon 443-749, Korea.*

[2]*Department of Chemistry, Korea University, 145, Anamro, Sungbuk-gu, Seoul 136-713, Korea.*

Table of Contents

Synthesis of SZn2-Mito. 6-Formyl-*N*-methyl-2-naphthylamine,[1] **A**,[2] **B**,[3] and (2-aminoethyl)triphenylphosphonium bromide[4] were prepared by the literature methods. Synthesis of other compounds is described below.

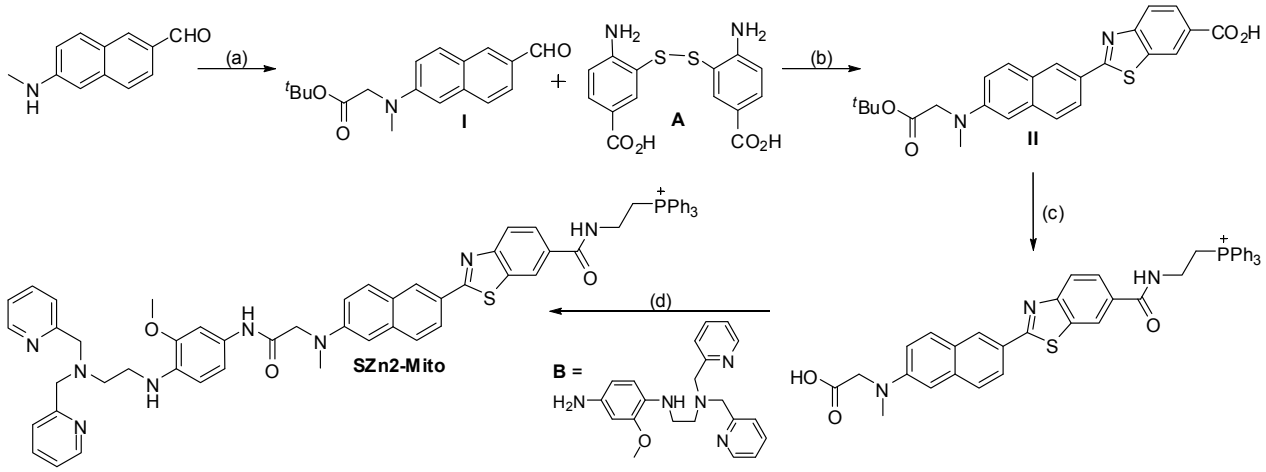

Scheme S1. Synthesis of SZnM. (a) *t*-butyl bromoacetate, proton-sponge, CH_3CN; (b) *p*-toluenesulfonic acid, DMF; (c) i: (2-aminoethyl)triphenylphosphonium bromide, DCC, HOBt, CH_2Cl_2; ii: CF_3CO_2H, CH_2Cl_2; (d) **B**, DCC, HOBt, DCM.

Synthesis of **I**. To a stirred solution of 6-formyl-*N*-methyl-2-naphthylamine (0.90 g, 4.9 mmol) and proton-sponge (1.2 g, 5.8 mmol) in dry CH_3CN (40 mL), *t*-butyl bromoacetate (1.05 mL, 7.3 mmol) was added and the reaction mixture was stirred at 80 °C under nitrogen atmosphere for 16 h. The solvent was evaporated and the resulting mixture was dissolved in CH_2Cl_2 (50 mL). The organic layer was washed several times with dilute H_2SO_4, separated and dried over $MgSO_4$. The solvent was removed under reduced pressure and the crude product was purified by column chromatography using hexane/ethyl acetate (2:1) as the eluent to give the brown solid. Yield: 1.0 g (68 %); m.p. 83 °C ; ^{1}H NMR (400 MHz, $CDCl_3$): δ 9.93 (s, 1H), 8.01 (d, J = 1.4 Hz, 1H), 7.76 (dd, J = 8.6, 1.4 Hz, 1H), 7.68 (d, J = 9.2 Hz, 1H), 7.57 (d, J = 8.6 Hz, 1H), 6.99 (dd, J = 9.2, 2.8 Hz, 1H), 6.78 (d, J = 2.8 Hz, 1H), 4.02 (s, 2H), 3.08 (s, 3H), 1.40 (s, 9H). ^{13}C NMR (100 MHz, $CDCl_3$): δ 191.2, 169.1, 149.1, 138.2, 134.5, 130.5, 126.7, 125.1, 123.0, 115.5, 105.6, 81.6, 54.9, 39.6, 28.0.

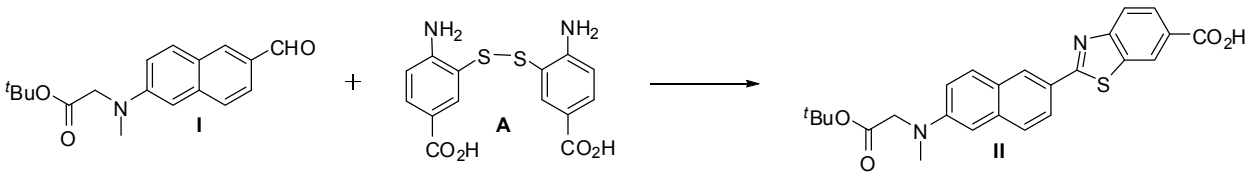

Synthesis of **II**. Compound **I** (0.50 g, 1.7 mmol), **A** (0.84 g, 2.5 mmol) and *p*-toluenesulfonic acid monohydrate (0.16 g, 0.84 mmol) were dissolved in DMF (10 mL) and the reaction mixture was stirred at 90 °C under nitrogen atmosphere for 18 h. After cooling to room temperature, distilled water was added. The product was collected by filtration, washed with water, and purified by crystallization from ethanol. Yield: 0.66 g (87 %); m.p. 260 °C; ^{1}H NMR (400 MHz, $CDCl_3$): δ 8.63 (s, 1H), 8.43 (d, J = 1.6 Hz, 1H), 8.16 (dd, J = 8.8 Hz, J = 1.6 Hz, 1H), 8.08 (dd, J = 8.8 Hz, J = 1.6 Hz, 1H), 8.04 (d, J = 8.8 Hz, 1H), 7.83 (d, J = 8.8 Hz, 1H), 7.72 (d, J = 8.8 Hz, 1H), 7.12 (dd, J = 8.8, 1.6 Hz, 1H), 6.90 (d, J = 1.6 Hz, 1H), 4.12 (s, 2H), 3.21 (s, 3H), 1.43 (s, 9H). ^{13}C NMR (100 MHz, $CDCl_3$): δ 171.5, 169.3, 167.6, 156.8, 148.4, 136.6, 134.5, 130.0, 127.7, 127.6, 127.3, 126.9, 126.5, 125.9, 124.6, 123.8, 122.0, 116.1, 105.7, 81.7, 55.1, 28.2.

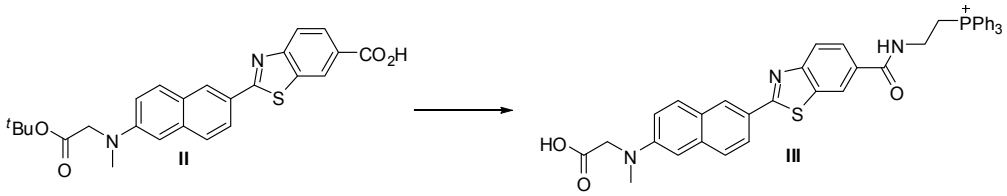

Synthesis of **III**. Compound **II** (0.30 g, 0.67 mmol), 1,3-dicyclohexyl carbodiimide (DCC, 0.17 g, 0.80 mmol) and 1-hydroxybenzotriazole (0.11 g, 0.80 mmol) were dissolved in dry CH_2Cl_2 (2 mL) and the reaction mixture was stirred at room temperature under nitrogen atmosphere for 1 h. To this mixture, (2-aminoethyl)triphenylphosphonium bromide (0.26 g, 0.67 mmol) was added and the reaction mixture was stirred for 16 h. The solvent was evaporated and the mixture was dissolved in CH_3CN. The byproduct urea was removed by filtration and the filtrate was concentrated under reduced pressure. The crude product was purified by column chromatography using 30 % methanol in $CHCl_3$ as the eluent to give foam like solid. Yield: 0.1 g (27 %); m.p. 123 °C. ^{1}H NMR (400 MHz, $CDCl_3$): δ 9.37 (br t, 1H, amide-NH), 8.55 (d, J = 1.6 Hz, 1H), 8.29 (d, J = 1.6 Hz, 1H), 8.09 (dd, J = 8.8, 1.6 Hz, 1H), 7.96-7.90

(m, 2H), 7.74-7.53 (m, 17H), 7.01 (dd, J = 9.2, 2.0 Hz, 1H), 6.80 (d, J = 2.0 Hz, 1H), 4.01 (s, 2H), 3.97-3.87 (m, 4H), 3.10 (s, 3H), 1.35 (s, 9H). ^{13}C NMR (100 MHz, $CDCl_3$): δ 171.4, 169.7, 166.9, 156.4, 148.5, 136.7, 135.2, 135.3, 134.7, 133.7, 133.6. 130.7, 130.5, 129.5, 127.8, 127.0, 126.9, 126.3, 124.9, 122.3, 122.1, 118.3, 117.4, 106.1, 82.1, 55.5, 40.2, 34.1, 28.4. ^{31}P NMR (400 MHz, $CDCl_3$): δ 21.85 ppm.

A solution of this intermediate (0.098 g, 0.12 mmol) and trifluoroacetic acid (1 mL) in CH_2Cl_2 (3 mL) was stirred at room temperature. The solvent was evaporated and diethyl ether was added. The precipitate obtained was filtered off and washed with diethyl ether. Yield: 0.075 g (82 %); m.p. 123 °C. ^{1}H NMR (400 MHz, $CDCl_3$/DMSO-d_6): δ 9.62 (br t, 1H, amide-NH), 8.54 (d, J = 1.6 Hz, 1H), 8.38 (d, J = 1.6 Hz, 1H), 8.08-7.80 (m, 3H), 7.84-7.66 (m, 17H), 7.11 (dd, J = 9.2, 2.0 Hz, 1H), 6.90 (d, J = 2.0 Hz, 1H), 4.18 (s, 2H), 3.94-3.90 (m, 4H), 3.20 (s, 3H). ^{13}C NMR (100 MHz, DMSO-d_6): δ 172.3, 171.2, 166.5, 156.2, 149.4, 137.1, 135.6, 134.7, 134.3, 134.2, 130.9, 130.8, 130.7, 128.3, 127.5, 126.2, 126.1, 124.7, 122.6, 122.3, 119.3, 118.5, 117.1, 105.8, 79.7, 53.9, 34.3. ^{31}P NMR (400 MHz, $CDCl_3$): δ 21.85 ppm.

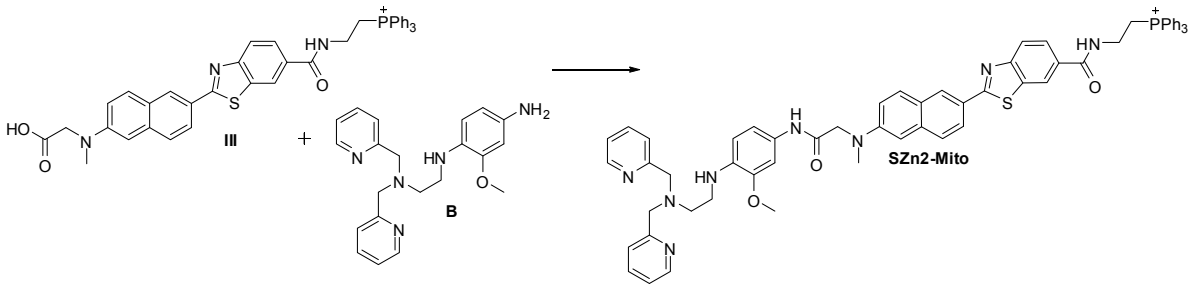

Synthesis of **SZn2-Mito**. Compound **III** (0.026 g, 0.072 mmol), DCC (0.019 g, 0.094 mmol) and 1-hydroxybenzotriazole (0.011 g, 0.086 mmol) were dissolved in CH_2Cl_2 (1 mL). The reaction mixture was stirred at room temperature for 1 h under nitrogen atmosphere. To this mixture, compound **B**^{ref} (0.065 g, 0.086 mmol) was added and the resulting mixture was stirred for 16 h. After the same work-up for **III**, the crude product was purified by column chromatography using 8 % methanol in $CHCl_3$ as the eluent to give **SZn2-Mito** as brown solid. Yield: 15 mg (33 %); m.p. 120 °C. ^{1}H NMR (400 MHz, $CDCl_3$): δ 9.62 (br t, 1H, amide-NH), 8.66 (d, J = 1.6 Hz, 1H), 8.50 (d, J = 4.4 Hz, 1H), 8.48 (d, J = 1.6

Hz, 1H), 8.19-8.12 (m, 3H), 8.05 (d, J = 8.8 Hz, 1H), 7.91-7.60 (m, 20H), 7.49 (d, J = 8.0 Hz, 1H), 7.25-7.09 (m, 5H), 6.76 (dd, J = 8.0, 2.0 Hz, 1H), 6.37 (d, J = 8.0 Hz, 1H), 4.11 (s, 2H), 4.09-4.00 (m, 4H), 3.89 (s, 4H), 3.85 (s, 3H), 3.24 (s, 3H), 3.16 (t, J = 6.2 Hz, 2H), 2.87 (t, J = 6.0 Hz, 2H). ^{13}C NMR (100 MHz, $CDCl_3$): δ 171.2, 167.8, 167.1, 159.3, 156.4, 149.0, 148.6, 146.9, 136.6, 136.3, 135.8, 135.3, 134.9, 133.8, 133.7, 130.7, 130.6, 129.7, 127.9, 127.7, 127.3, 127.1, 126.2, 125.3, 123.1, 122.2, 122.1, 118.4, 117.6, 116.8, 113.2, 109.8, 107.6, 103.8, 60.6, 59.3, 56.0, 53.2, 41.6, 40.5, 34.2, 30.1. ^{31}P NMR (400 MHz, $CDCl_3$): δ 21.79 ppm. HRMS (FAB^+): m/z calcd for $[C_{62}H_{58}N_8O_3PS]^+$: 1025.41, found: 1025.41.

Spectroscopic measurements. Absorption spectra were recorded on a S-3100 UV-Vis spectrophotometer and fluorescence spectra were obtained with FluoroMate FS-2 fluorescence spectrophotometer with a 1 cm standard quartz cell. The fluorescence quantum yield was determined by using coumarin 307 (Φ = 0.95 in MeOH) as the reference by the literature method.[5]

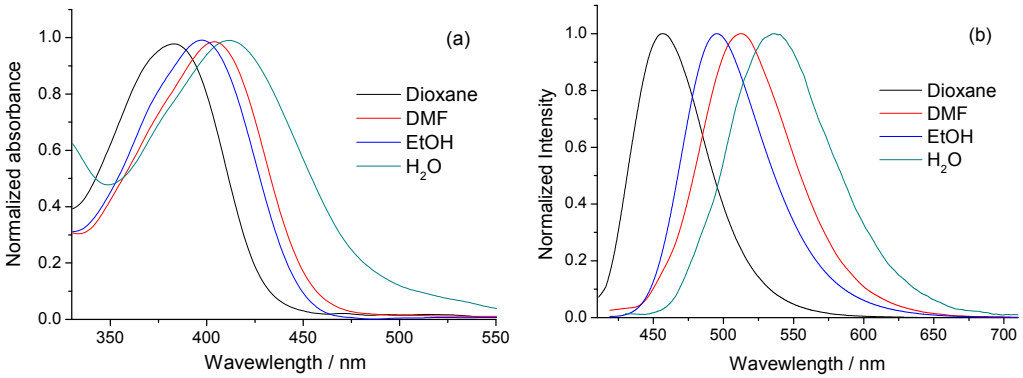

Figure S1. Normalized absorption (a) and emission (b) spectra of SZn2-Mito in 1,4-dioxane, DMF, EtOH, and buffer (50 mM HEPES, 100 mM KCl, 10 mM NTA, pH 7.4).

Table S1. Photophysical properties of SZn2-Mito in various solvents.

Solvent (E_T^N)[a]	$\lambda_{max}^{(1)}$, nm[b]	λ_{max}^{fl}, nm[c]	Φ[d]
Dioxane (0.164)	382	456	0.35
DMF (0.386)	405	512	0.05
EtOH (0.654)	397	495	0.17
Buffer (1.00)[e]	413	536	0.0048

a) The numbers in the parenthesis are normalized empirical parameter of solvent polarity.[6] b,c) λ_{max} of the one-photon absorption and emission spectra in nm. d) Fluorescence quantum yield, ± 15 %. e) HEPES buffer (50 mM HEPES, 100 mM KCl, 10 mM NTA, pH 7.4). The E_T^N value is for water.

Water solubility. Small amount of dye was dissolved in DMSO to prepare the stock solutions (1.0×10^{-2} M). The solution was diluted to ($6.0 \times 10^{-3} \sim 6.0 \times 10^{-5}$) M and added to a cuvette containing 3.0 mL of buffer (50 mM HEPES, 100 mM KCl, 10 mM NTA, pH 7.4) by using a micro syringe. In all cases, the concentration of DMSO in H_2O was maintained to be 0.2 %.[7] The plots of fluorescence intensity against the dye concentration were linear at low concentration and showed downward curvature at higher concentration (Figure S2). The maximum concentration in the linear region was taken as the solubility. The solubility of SZn2-Mito in buffer was ~ 2.0 μM.

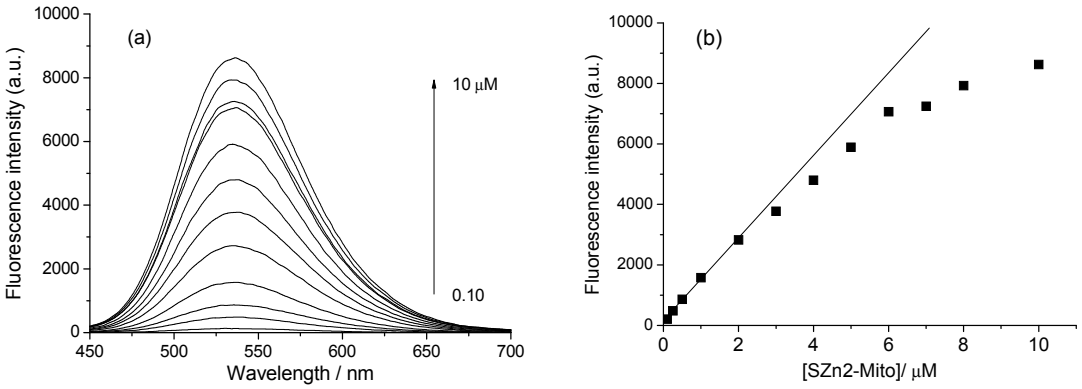

Figure S2. (a) One-photon fluorescence spectra and (b) plot of fluorescence intensity against dye concentration for SZn2-Mito in buffer (50 mM HEPES, 100 mM KCl, pH 7.4). The excitation wavelength was 413 nm.

Table S2. Photophysical data for SZn2-Mito in buffer.[a]

Compd	$\lambda_{max}^{(1)}$ (10^{-4} ε) [b]	λ_{max}^{fl} [c]	Φ[d]	K_d^{OP} / K_d^{TP} [e]	*FEF* [f]	$\lambda_{max}^{(2)}$ [g]	Φδ[h]
SZn2-Mito	413(1.85)	536	0.0048	1.4/1.4	70(68)	nd	nd
SZn2-Mito/Zn^{2+}	395(2.10)	536	0.33			750	155

a) SZn2-Mito was measured in HEPES buffer (50 mM HEPES, 100 mM KCl, 10 mM NTA, pH 7.4) in the absence and presence (47 nM) of free Zn^{2+} unless otherwise noted. b) λ_{max} of the one-photon absorption spectra in nm. The numbers in parentheses are molar extinction coefficients in $M^{-1}cm^{-1}$. c) λ_{max} of the one-photon emission spectra in nm. d) Fluorescence quantum yield, ± 15 %. e) Dissociation constants for Zn^{2+} in nM measured by one- (K_d^{OP}) and two-photon (K_d^{TP}) processes, ± 10 %. f) Fluorescence enhancement factor, $(F - F_{mim})/F_{min}$, measured by one-photon processes. The number in parentheses is measured by two-photon process. g) λ_{max} of the two-photon excitation spectra in nm. h) Two-photon action cross section in 10^{-50} cm^4s/photon (GM), ± 15%.

Determination of Apparent Dissociation Constants. A series of HEPES (4-(2-hydroxyethyl)-1-piperazineethanesulfonic acid) buffer solutions (50 mM HEPES, pH 7.4, 0.1 M KCl) containing various amounts of $ZnSO_4$ (0 ~ 9.5 mM) and 10 mM of NTA (Nitrilotriacetic acid) were prepared. The $[Zn^{2+}]_{free}$ was calculated from the $K_{Zn\text{-}NTA}^{app}$, $[NTA]_{total}$, and $[Zn^{2+}]_{total}$ using Eq (1).[8,9]

$$[Zn^{2+}]_{free} = [Zn^{2+}]_{total} / (\alpha_{Zn} \times K_{Zn\text{-}NTA}^{app} \times [NTA]_{free}) \qquad (1)$$

Where,

$$K_{Zn\text{-}NTA}^{app} = K_{Zn\text{-}NTA} / \alpha_{Zn}\alpha_{NTA},$$

$$\alpha_{Zn} = 1 + 10^{(pH - pK_1)} + 10^{(2pH - pK_1 - pK_2)} + 10^{(3pH - pK_1 - pK_2 - pK_3)} \ldots,$$

$$\alpha_{NTA} = 1 + 10^{(pK_1 - pH + 0.11)} + 10^{(pK_1 + pK_2 - 2pH + 0.22)} + 10^{(pK_1 + pK_2 + pK_3 - 3pH + 0.33)} \ldots,$$

and

$$[NTA]_{free} = [NTA]_{total} - [Zn^{2+}]_{total}$$

Thus,

$$K_{Zn\text{-}NTA}^{app} = \frac{K_{Zn\text{-}NTA}(1 + 10^{(pK_{Zn\text{-}NTA} - pH)})}{(1 + 10^{(pH - pK_{Zn})})(1 + 10^{(pK_1 - pH)} + 10^{(pK_1 + pK_2 - 2pH)})}$$

The stability constant for the Zn^{2+} complex of NTA ($K_{Zn\text{-}NTA}$) was taken from ref. 10. Thus, for NTA (pH 7.4, 0.1 M KCl, 25 °C), pK_1 = 9.73, pK_2 = 2.49, pK_3 = 1.89, log $K_{Zn\text{-}NTA}$ = 10.66.

All protonation constants must be corrected upward by 0.11 when worked out in 0.1 M ionic strength. $[NTA]_{total}$ was set at 10 mM, and $[Zn^{2+}]_{total}$ was varied from 0-9.4 mM.

The calculated $[Zn^{2+}]_{free}$ concentration of each solution is:

$[Zn^{2+}]_{total}$ (mM)	0.50	1.00	1.50	2.00	2.50	3.00	3.50	4.99	5.99	6.98	7.98	8.97	9.40
$[Zn^{2+}]_{free}$ (nM)	0.14	0.46	0.66	0.87	1.10	1.14	1.80	2.60	3.90	6.10	10.0	22.0	47.0

To determine the apparent dissociation constants for the Zn^{2+} complex of probes, the fluorescence titration curves (Figure S3b) was obtained and fitted to Eq 2 (Figure S3c).[11,12]

$$F = F_0 + (F_{max} - F_0)\frac{[Zn^{2+}]_{free}}{K_d + [Zn^{2+}]_{free}} \qquad (2)$$

where F is the fluorescence intensity, F_{max} is the maximum fluorescence intensity, F_0 is the fluorescence intensity in the absence of Zn^{2+}, and $[Zn^{2+}]_{free}$ is the free Zn^{2+} concentration. The K_d value that best fits the titration curve (Figure S3c) with Eq 2 was calculated by using the program, Origin 7.5.

In order to determine the K_d^{TP} for the two-photon process, the TPEF spectra were obtained with CCD detector. They were excited by a mode-locked titanium-sapphire laser source (Coherent Chameleon, 90 MHz, 200 fs) set at wavelength 750 nm and output power 1343 mW, which corresponded to approximately 200 mW average power in the focal plane. The TPEF titration curves (Figure 1a) were obtained and fitted to Eq 2 (Figure S3c).

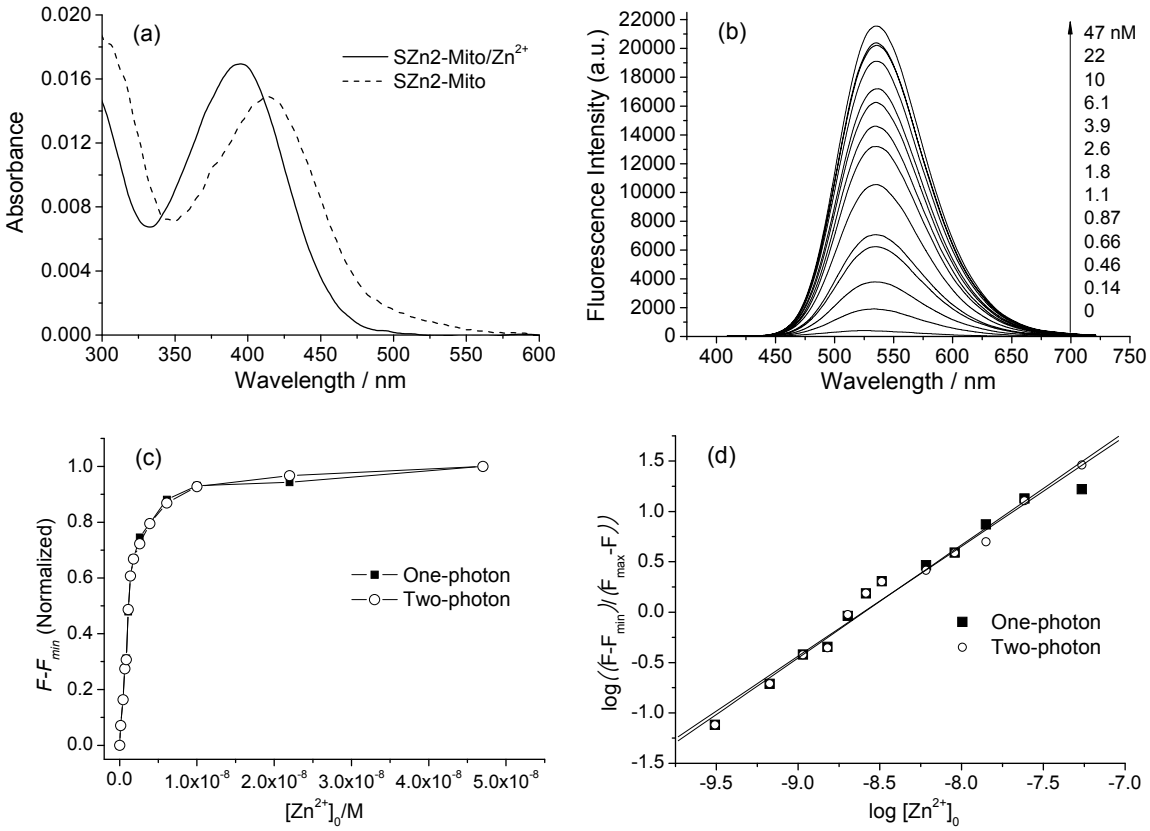

Figure S3**.** (a) One-photon absorption, and (b) emission spectra of SZn2-Mito (50 mM HEPES, 100 mM KCl, 10 mM NTA, pH 7.4) in the presence of free Zn^{2+} (0–47 nM). (c) One- (■) and two-photon (○) fluorescence titration curve for the complexation of SZn2-Mito with free Zn^{2+} (0–47 nM). (d) Hill plots for the complexation of SZn2-Mito with free Zn^{2+} (0–47 nM). The excitation wavelengths for one- and two-photon processes were 395 and 750 nm, respectively.

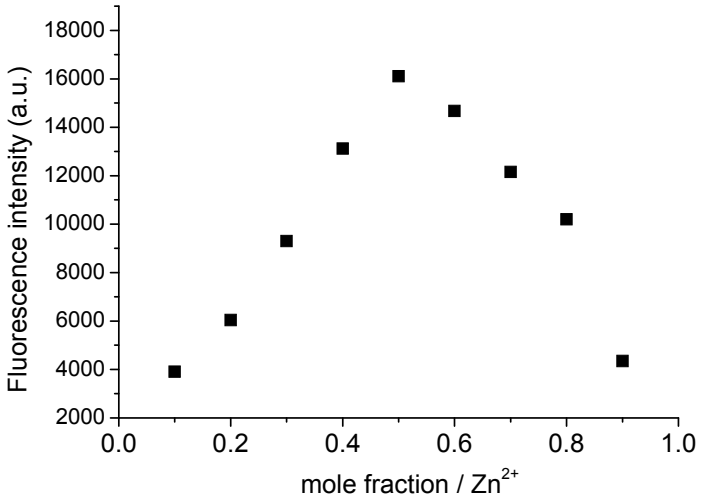

Figure S4. Job's plot of SZn2-Mito with Zn^{2+} in HEPES buffer (50 mM HEPES, 100 mM KCl, pH 7.4). Solutions of SZn2-Mito and $ZnSO_4$ in different mole fractions were prepared in appropriate ratios while maintaining the total concentration to 1 μM. The plot of the fluorescence intensity vs the mole fraction of Zn^{2+} shows a maximum when the mole fraction is 0.5, indicating the formation of a 1:1 complex.

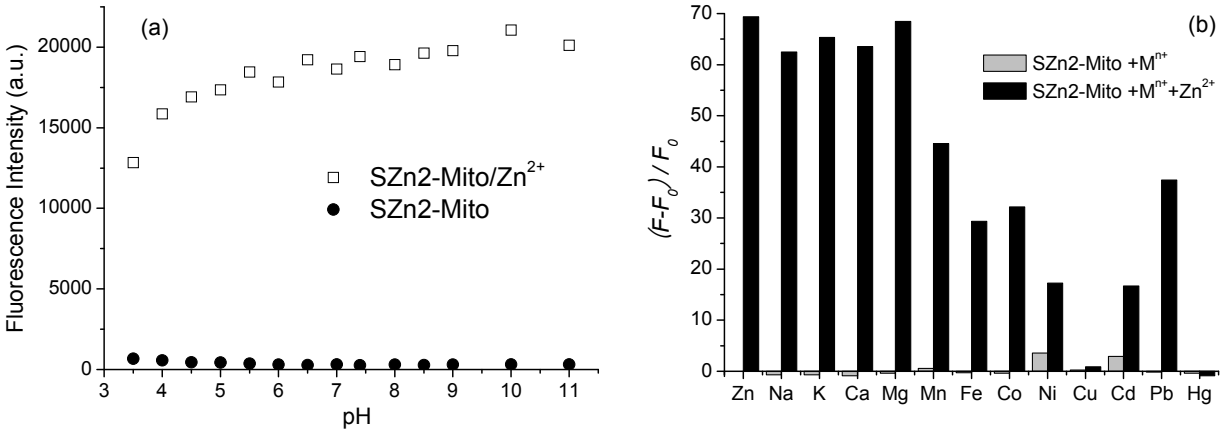

Figure S5. (a) Effect of the pH on the one-photon fluorescence intensity of 1 μM SZn2-Mito in the absence (○) and presence of 1.0 μM (■) of free Zn^{2+} in HEPES buffer (50 mM HEPES, 100 mM KCl, 10 mM NTA, pH 7.4). The data at $[Zn^{2+}]$ = 0 μM were determined by adding 10 mM NTA. The excitation wavelength was 395 nm. (b) The relative fluorescence intensity of 1.0 μM of SZn2-Mito in the presence of 1.0 mM for Na^{+}, K^{+}, Ca^{2+}, Mg^{2+}; 1.0 μM for Mn^{2+}, Fe^{2+}, Co^{2+}, Ni^{2+}, Cu^{2+}, Cd^{2+}, Pb^{2+}, Hg^{2+} (gray bars) followed by addition of 1.0 μM of Zn^{2+} (filled bars) in HEPES buffer.

Measurement of Two-Photon Cross Section. The two-photon cross section (δ) was determined by using femto second (fs) fluorescence measurement technique as described.[13] SZn2-Mito (1.0×10^{-6} M) was dissolved in 50 mM HEPES buffer (100 mM KCl, 10 mM NTA, pH 7.4) and the two-photon induced fluorescence intensity was measured at 720−900 nm by using rhodamine 6G as the reference, whose two-photon property has been well characterized in the literature.[14] The intensities of the two-photon induced fluorescence spectra of the reference and sample emitted at the same excitation wavelength were determined. The TPA cross section was calculated by using $\delta = \delta_r(S_s\Phi_r\phi_r c_r)/(S_r\Phi_s\phi_s c_s)$: where the subscripts *s* and *r* stand for the sample and reference molecules. The intensity of the signal collected by a CCD detector was denoted as *S*. Φ is the fluorescence quantum yield. ϕ is the overall fluorescence collection efficiency of the experimental apparatus. The number density of the molecules in solution was denoted as *c*. δ_r is the TPA cross section of the reference molecule.

Cell Culture. HeLa human cervical carcinoma cells (ATCC, Manassas, VA, USA) were cultured in DMEM (WelGene Inc, Seoul, Korea) supplemented with 10 % FBS (WelGene), penicillin (100 units/ml), and streptomycin (100 μg/mL). Two days before imaging, the cells were passed and plated on glass-bottomed dishes (MatTek). All the cells were maintained in a humidified atmosphere of 5/95 (v/v) of CO_2/air at 37 °C. For labeling, the growth medium was removed and replaced with DMEM without FBS. The cells were treated and incubated with 1.0 μL of 1 mM SZn2-Mito in DMSO stock solution (1.0 μM SZn2-Mito) at 37 °C under 5 % CO_2 for 30 min. The cells were washed three times with phosphate buffered saline (PBS; Gibco) and then imaged after further incubation in colorless serum-free media for 15 min.

Two-Photon Fluorescence Microscopy. Two-photon fluorescence microscopy images of SZn2-Mito-labeled cells and tissues were obtained with spectral confocal and multiphoton microscopes (Leica TCS SP2) with ×10, ×20, ×40 dry and ×100 oil objectives, numerical aperture (NA) = 0.30, 0.50, 0.75, and

1.30. The two-photon fluorescence microscopy images were obtained with a DM IRE2 Microscope (Leica) by exciting the probes with a mode-locked titanium-sapphire laser source (Coherent Chameleon, 90 MHz, 200 fs) set at wavelength 750 nm and output power 1343 mW, which corresponded to approximately 10 mW average power in the focal plane. To obtain images, internal PMTs were used to collect the signals in an 8 bit unsigned 512 × 512 and 1024 × 1024 pixels at 800 and 400 Hz scan speed, respectively.

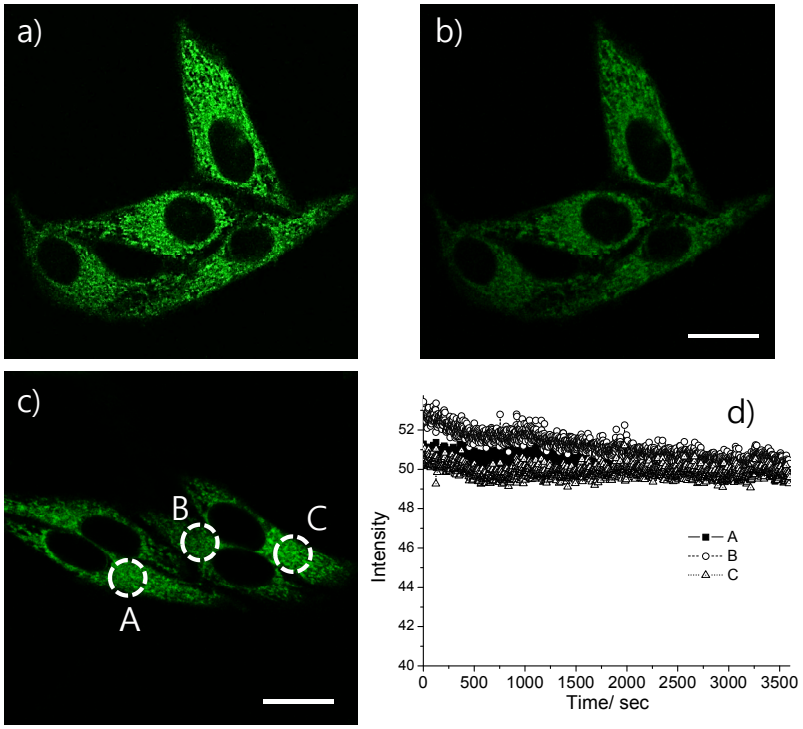

Figure S6. (a,b,c) TPM images of HeLa cells labeled with 1.0 μM SZn2-Mito, before (a) and after (b) addition of 20 μM TPEN to the imaging solution. (d) The relative TPEF intensity from the A-C in (c) as a function of time. The digitized intensity was recorded with 1.63 sec intervals for the duration of one hour using *xyt* mode. The TPEF intensities were collected at 450-600 nm upon excitation at 750 nm with fs pulse. Cells shown are representative images from replicate experiments (n = 5).

Photostability. Photostability of SZn2-Mito was determined by monitoring the changes in TPEF intensity with time at three designated positions of SZn2-Mito-labeled (1 μM) HeLa cells chosen without bias (Figure S6c). The TPEF intensity remained nearly the same for 1 hr (Figure S6d), indicating high photostability.

Detection window. The TPM image of freshly cultured HeLa cells labeled with 1.0 μM SZn2-Mito was bright. Moreover, the TP excited fluorescence (TPEF) spectrum from the red-circled domain in Figure S7 was symmetrical and slightly blue-shifted from that measure in HEPES buffer with emission maximum at ~490 nm (Figure S7). This indicates that the polarity of the probe environment is rather homogeneous and slightly more hydrophobic than that of HEPES buffer. Therefore, we have detected $[Zn^{2+}]_m$ by using the detection window at 400-600 nm.

For colocalization experiment, the emission spectra of SZn2-Mito and Mitotracker Red FM in the HeLa cells were compared. The detection windows for SZn2-Mito and Mitotracker Red FM were determined by considering two factors; i) the emission from the two probes should be separated as far as possible, ii) the emission intensities from the probes should be similar. The detection windows that meet above requirements were 450-550 (SZn2-Mito) and 600-700 nm (Mitotracker Red FM), respectively (Figure S7).

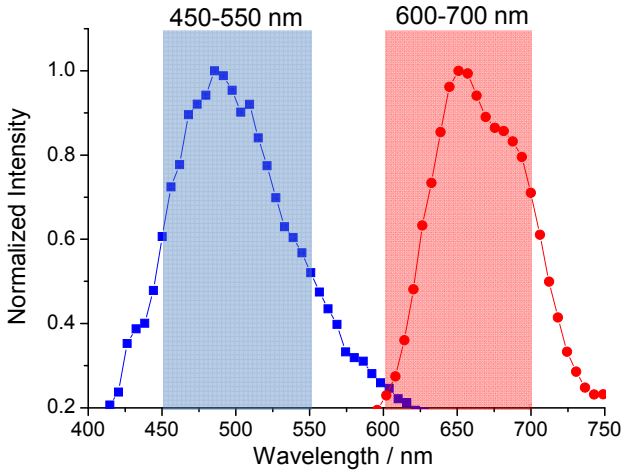

Figure S7. One and two-photon excited fluorescence spectra of SZn2-Mito (λ_{ex} = 750 nm) and Mitotracker Red FM (λ_{ex} = 544 nm) in HeLa cells, and the detection windows for SZn2-Mito (blue channel) and Mitotracker Red FM (red channel).

Cell viability. To confirm that the probe couldn't affect the viability of HeLa cells in our incubation condition, we used CCK-8 kit (Cell Counting Kit-8, Dojindo, Japan) according to the manufacture's protocol. The results are shown in Figure S8.

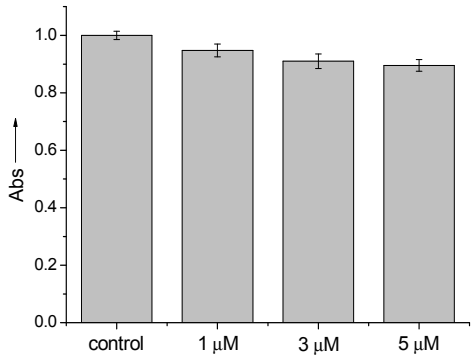

Figure S8. Viability of HeLa cells in the presence of SZn2-Mito as measured by using CCK-8 kit. The cells were incubated with SZn2-Mito for 2 hrs.

Effects of DTDP, Zn^{2+}/pyrithione, and CCCP. Stock solutions of 2,2′-dithiodipyridine (DTDP) and *m*-chlorophenylhydrazone (CCCP) were prepared by dissolving DTDP (2.0 mg) and CCCP (22 mg) in DMSO (1.0 mL). The solution of Zn^{2+}/pyrithione (1:1) was prepared by dissolving $ZnCl_2$ (14 mg) and pyrithione (13 mg) in cold water (1.0 mL). Each solution (1 μL) was diluted to 0.1 mL with ACSF and added to the imaging solution (0.9 mL) with a micropipette. The effects of Effects of DTDP, Zn^{2+}/pyrithione, and CCCP on the TPEF intensity are shown in Figures 2 and S9.

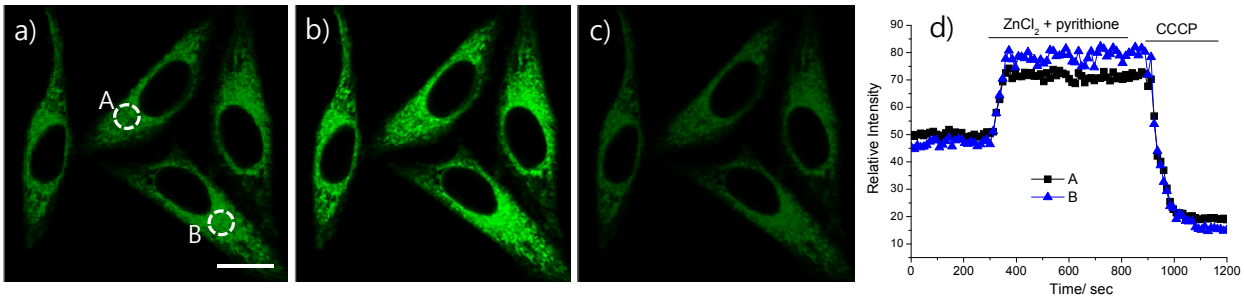

Figure S9. (a-c) TPM images of 1 μM SZn2-Mito-labeled HeLa cells, before (a) and after (b) addition of 100 μM Zn^{2+}/pyrithione (1:1) to the imaging solution. (c) After addition of 10 μM CCCP to (b). (d) The relative TPEF intensity of SZn2-Mito-labeled HeLa cells as a function of time. The TPEF intensities were collected at 400-600 nm upon excitation at 750 nm with fs pulse. Scale bar, 30 μm. Cells shown are representative images from replicate experiments (n = 5).

Preparation and Staining of fresh rat Hippocampal slices. Slices were prepared from the hippocampi of 2-weeks-old rat (SD). Coronal slices were cut into 400 μm-thick using a vibrating-blade microtome in artificial cerebrospinal fluid (ACSF; 138.6 mM NaCl, 3.5 mM KCl, 21 mM $NaHCO_3$, 0.6 mM NaH_2PO_4, 9.9 mM D-glucose, 1 mM $CaCl_2$, and 3 mM $MgCl_2$). Slices were incubated with 2 μL from 10 mM stock solution of SZn2-Mito in DMSO (total 20 μM SZn2-Mito) in ACSF bubbled with 95% O_2 and 5% CO_2 for 30 min at 37 °C. Slices were then washed three times with ACSF and transferred to glass-bottomed dishes (MatTek) and observed in a spectral confocal multiphoton microscope. The TPM images of fresh rat Hippocampal slice labeled with 20 μM SZn2-Mito obtained at 100–200 μm depth are shown in Figure S10.

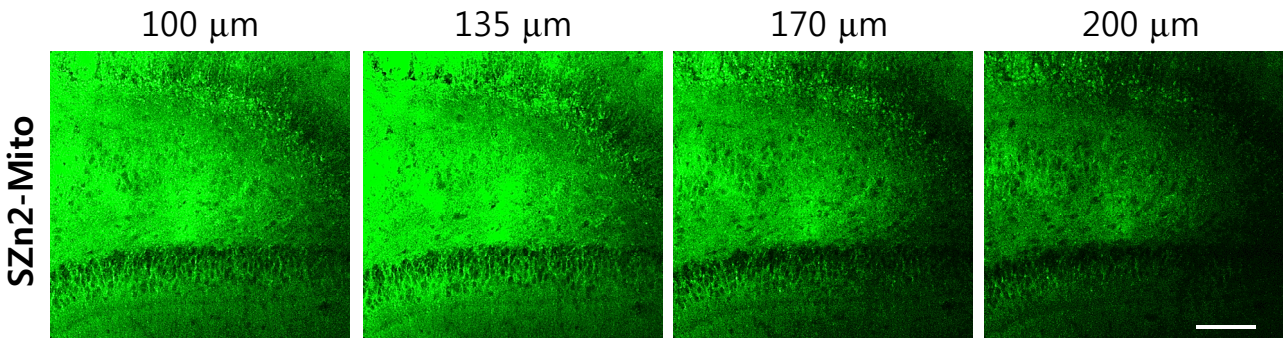

Figure S10. TPM images of rat hippocampal slices labeled with 20 μM SZn2-Mito for 1.0 h. The images show the hilus (H) of the dentate gyrus (DG) region by magnification at 20×. Scale bar: 75 μm.

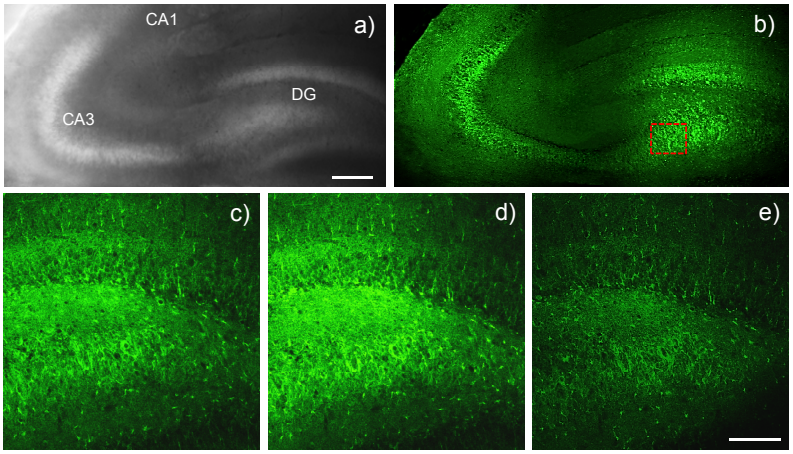

Figure S11. Images of a rat hippocampal slice stained with 20 μM SZn-Mito for 1 h. (a) Bright-field images of the CA1-CA3 regions as well as dentate gyrus (DG) at 10x magnification. (b) 10 TPM images along the *z*-direction at the depths of 100-200 μm were accumulated. (c-e) Magnification at 40x in the DG regions [red box in (b)] at a depth of ~100 μm (c) before and (d) after addition of 150 μM DTDP to the imaging solution and (e) after addition of 10 μM CCCP to (d). Scale bars: (a) 300 and (e) 75 μm. The TPM images for SZn-Mito are taken from Ref 15.

References

(1) Kim, H. M.; Jeong, B. H.; Hyon, Ju-Y.; An, M. J., Seo, M. S.; Hong, J. H.; Lee, K. J.; Kim, C. H.; Joo, T.; Hong, Seok-C.; Cho, B. R. *J. Am. Chem. Soc.* **2008**, *130*, 4246-4247.

(2) Serdons, K.; Terwinghe, C.; Vermaelen, P.; Laere, K. V.; Kung, H.; Mortelmans, L.; Bormans, G.; Verbruggen, A. *J. Med. Chem.* **2009**, *52,* 1428–1437.

(3) Kim, H. M.; Seo, M. S.; An, M. J.; Hong, J. H.; Tian, Y. S.; Choi, J. H.; Kwon, O.; Lee, K. J.; Cho, B. R. *Angew. Chem. Int. Ed.* **2008**, *47*, 5167.

(4) Maryanoff, B. E.; Reitz, A. B.; Duhl-Emswiler, B. A. *J Am. Chem. Soc.* **1985**, *107*, 217-226.

(5) Demas, J. N.; Crosby, G. A. *J. Phys. Chem.* **1971**, *75*, 991-1024.

(6) Reichardt, C. *Chem. Rev.* **1994**, *94*, 2319-2358.

(7) Kim, H. M.; Choo, H.-J.; Jung, S.-Y.; Ko, Y.-G.; Park, W.-H.; Jeon, S.-J.; Kim, C. H.; Joo, T.; Cho, B. R. *ChemBioChem* **2007**, *8*, 553-559.

(8) Fahrni, C. J.; O'Halloran, T. V. *J. Am. Chem. Soc.* **1999**, *121*, 11448–11458.

(9) Taki, M.; Wolford, J. L.; O'Halloran, T. V. *J. Am. Chem. Soc.* **2004**, *126*, 712–713.

(10) Martell, A. E.; Smith, R. M. *NIST Critical Stability Constants of Metal Complexes. NIST Standard Reference Database 46, Version 7.0, 2003*.

(11) Hirano, T.; Kikuchi, K.; Urano, Y.; Higuchi, T.; Nagano, T. *J. Am. Chem. Soc.* **2000**, *122*, 12399-12400.

(12) Hirano, T.; Kikuchi, K.; Urano, Y.; Nagano, T. *J. Am. Chem. Soc.* **2002**, *124*, 6555-6562.

(13) Lee, S. K.; Yang, W. J.; Choi, J. J.; Kim, C. H.; Jeon, S.-J.; Cho, B. R. *Org. Lett.* **2005**, *7*, 323-326.

(14) Makarov, N. S.; Drobizhev, M.; Rebane, A. *Optics Express*. **2008**, *6*, 4029-4047.

(15) G. Masanta, C. S. Lim, H. J. Kim, J. H. Han, H. M. Kim and B. R. Cho, *J. Am. Chem. Soc.* **2011**, *133*, 5698.